Predefined-Time Neural Adaptive Quantized Self-Triggered Control With Appointed Performance for a 2-DOF Helicopter System

Xiaona Song, *Senior Member, IEEE*, Longbo Chu, Zhijia Zhao, *Member, IEEE*, Shuai Song, *Member, IEEE*, and Keum-Shik Hong, *Life Fellow, IEEE*

***Abstract*—This article investigates the predefined-time neural adaptive self-triggered quantized control design for a two-degree of freedom (2-DOF) helicopter system with appointed tracking performance. To begin with, a fixed-time performance function is integrated into the predefined-time dynamic surface control (PTDSC) framework, and the transient fluctuations of the tracking error can be effectively constrained by the performance function. Then, a neural adaptive self-triggered quantized resilient controller is designed, where the self-triggered mechanism and input quantization are incorporated into to recursive control design to reduce the bandwidth consumption. Furthermore, the obtained stability results have proved that the designed controller ensures all the signals in the closed-loop system are practical predefined-time bounded (PPTB), and the tracking errors can be strictly confined to a region with preset transient and steady-state performance, even under limited communication resources. Finally, the simulation results demonstrate the effectiveness of the proposed control scheme.**

***Index Terms*—Adaptive predefined-time control, 2-DOF helicopter systems, input quantization, preset transient and steady-state performance, self-triggered mechanism.**

Received 3 September 2024; revised 20 November 2024; accepted 1 January 2025. Date of publication 20 January 2025; date of current version 20 June 2025. This work was supported in part by the National Natural Science Foundation of China under Grant 62203153 and Grant 62473130, part by the Joint Fund of Science and Technology R&D Plan of Henan Province for Young Scientists under Grant 235200810105, in part by the Application Research Project of the Joint Fund of Science and Technology R&D Plan of Henan Province under Grant 235200810105, in part by the Key Scientific Research Projects of Higher Education Institutions in Henan Province under Grant 22A413001, in part by Top Young Talents in Central Plains under Grant Yuzutong (2021) 44, in part by the Technology Innovative Teams in University of Henan Province under Grant 23IRTSTHN012, and in part by the National Research Foundation of Korea funded by the Ministry of Science and ICT, Korea under Grant Number IRIS-2023-00207954. The review of this article was coordinated by Prof. Xianbin Cao. *(Corresponding author: Shuai Song.)*

Xiaona Song is with the School of Information Engineering, Henan University of Science and Technology, Luoyang 471000, China, and also with the Henan Key Laboratory of Robot and Intelligent Systems, Henan University of Science and Technology, Luoyang 471000, China (e-mail: xiaona_97@163.com).

Longbo Chu and Shuai Song are with the School of Information Engineering, Henan University of Science and Technology, Luoyang 471000, China (e-mail: longbo_2023@163.com; songshuai_1010@163.com).

Zhijia Zhao is with the School of Mechanical and Electrical Engineering, Guangzhou University, Guangzhou 510006, China (e-mail: zhjzhaoscut@163.com).

Keum-Shik Hong is with the School of Mechanical Engineering, Pusan National University, Busan 46241, South Korea (e-mail: kshong@pusan.ac.kr).

Digital Object Identifier 10.1109/TVT.2025.3531513

I. Introduction

In RECENT years, the unmanned helicopters have been extensively used in marine supervision, material transportation, forest fire suppression, and other fields due to its advantages of vertical take-off and landing, flexible and convenient operation, hovering flight, and so on [1]. The helicopter is essentially a multiple-input multiple-output (MIMO) nonlinear system with forcefully coupling and uncertainties [2], which makes the control design more challenging. As a result, various research have been made to study the stability and control design of helicopter systems. An adaptive backstepping control approach was proposed for a 2-DOF helicopter in [3]. Furthermore, various intelligent approximators including fuzzy system, neural networks, and their combination have been gradually introduced into recursive control design of helicopter systems for dealing with the system uncertainties [4], [5], [6]. Among them, a robust fuzzy flight control approach was established for unknown 2-DOF helicopter systems (2-DOFHSs) in [4], where the stability criteria were derived by means of linear matrix inequality technique. In [6], an adaptive neural tracking control strategy was developed for a constrained 2-DOFHS, which ensures boundedness of all the signals in the closed-loop system (CLS). Furthermore, a neural DSC design was performed for an underactuated helicopter system in [7], which avoided the potential computation problem exposed in [5], [6]. It is noted that the convergence of tracking errors was not addressed in the papers above, apart from the boundedness of the closed-loop signals.

Considering the finite-time control (FTC) possesses good attributes like better steady-state precision and faster convergence rate, a number of FTC designs have been reported [8], [9], [10], [11]. For instance, an finite-time output-feedback control scheme was introduced in [8], which can ensure the finite-time stability of the entire CLS consisting of a position subsystem and an attitude subsystem. In [11], a neural adaptive finite-time control design with event-triggered mechanism was proposed for a 2-DOFHS. A common feature of the foregoing results is that the settling time of the CLS heavily depends on the prior knowledge about the system's initial conditions, which also implies that the obtained results are conservative to some extent. To handle this issue, the fixed-time stability concept [12] was introduced to controller design of different types of helicopter systems [13], [14], [15]. In [14], the fixed-time adaptive quantized control

problem was addressed for constrained 2-DOFHSs, where the preassigned constraint on system outputs was achieved by establishing a logarithmic barrier Lyapunov function. In [15], a reinforcement learning-based fixed-time attitude control scheme was proposed for 2-DOF helicopters, where the actor-critic networks were adopted to update the weights. Nevertheless, in the above-mentioned results, the upper bound of settling time was determined by a complicated function of system parameters, so it was difficult for designers to obtain a specific settling time in advance. For this purpose, various efforts have been made to achieve the predefined-time (PT) stability of nonlinear systems [16], [17], [18], [19], [20]. However, it should be emphasized that the adaptive PT control for helicopter systems with appointed tracking performance has not been outright studied so far.

The prescribed performance control (PPC), first reported in [21], has paid considerable attention to receive in the past decades due to its obvious advantage of flexibility in the adjustment of transient and steady-state responses. Especially for helicopter systems, some notable results have been successively reported [22], [23], [24]. In [22], a fractional-order observer-based tracking control design with performance assurance was presented for an unmanned autonomous helicopter, where an exponential performance function (EPF) was employed to achieve the specific constraints on tracking errors. Noted that the above EPF laid particular attention on steady-state performance, making the convergence of the tracking error may not meet the practical application requirements. To balance the system's steady-state and transient performance, a reinforcement learning-based prescribed performance control scheme was proposed for 2-DOF helicopters in [24]. However, it should be noticed that the above-mentioned PPC methods were primarily dependent on the time-triggered control (TTC) method, and the methods would undoubtedly give rise to unnecessary waste of communication resources. Therefore, how to balance the tracking performance and control consumption is still a challenging issue for helicopter flight control.

Quantized control has been widely recognized as an effective method for relieving network transmission burden owing to the practical significance in digital and networked control systems [25], [26], [27], [28]. In [26], an adaptive quantized backstepping control strategy was proposed to achieve attitude control for MIMO rigid body systems, where a quantizer was employed in communication channels to decrease the communication burden as possible. For 2-DOF helicopter systems subject to actuator failures, a neurally resilient quantized control design was established in [28], which makes sure the boundedness of all the closed-loop signals even when the actuators encounter the unexpected faults suddenly. On the other hand, various efforts have been devoted to studying control issue under limited transmission bandwidth from the perspective of signal transmission mechanism. To this end, a large number of event-triggered mechanisms have been incorporated into controller design of different types of systems for achieving the transmission of control signals in demand [29], [30], [31]. In [29], a dynamic event-triggered control design was developed to address the path-following issue of unmanned surface vehicles, where the traditional triggering mechanism with fixed threshold was replaced with a dynamic triggering mechanism with adaptive parameter to release bandwidth burden. By synthesizing the characteristics of cyberattacks, an event-driven secure control scheme was developed for a 2-DOFHS against DoS attacks in [31]. However, it should be noted that the above-mentioned ETC methods need to continuously monitor and estimate whether the events have been triggered, which undoubtedly imposed more or less restrictions on practical applications. Therefore, developing a communication resource-efficient control design for a 2-DOFHS remains a challenging issue so far.

Inspired by the aforesaid insights, a PT neural adaptive quantized self-triggered control method is developed for a 2-DOFHS with specific performance requirements. The main contributions of this article are as follows.

(i) Compared with some existing PPC results [32], [33], an improved fixed-time performance function is incorporated into the recursive control design, which steer the tracking error to converge into a small region of zero at a specified time with better transient and steady state performance.

(ii) A communication resource-efficient control design is proposed by integrating input quantization and self-triggered mechanism, which can greatly enhance the utilization of communication resources in comparison to single quantized control design [25], [26]. Additionally, the rigorous condition on continuous monitoring for the triggering rules existing in the ETC results [31], [33], [34] is fully removed.

(iii) Distinct from the existing backstepping control design presented in [23], [28], [33], a modified DSC design involving a predefined-time filter is developed, which not only can eliminate the computational complexity exposed in the traditional backstepping framework, but also can guarantee that the filter error converges to a small neighborhood within a PT.

Notations: In this manuscript, $\|\cdot\|$ represents the Euclidian 2-norm and $\mathrm{diag}(\cdot)$ means the diagonal matrix. Furthermore, N^+ stands for the set of positive integers. For a vector $a = [a_1, a_2]^T$ and a constant γ, then $\mathrm{sig}^\gamma(a)$ is denoted as $\mathrm{sig}^\gamma(a) = [|a_1|^\gamma \mathrm{sig}(a_1), |a_2|^\gamma \mathrm{sig}(a_2)]^T$, in which $\mathrm{sig}(\cdot)$ stand for the sign function.

II. Problem Formulation

A. Model Description

Consider a 2-DOF helicopter model in Fig. 1, which can be described by the following equations:

$$\begin{cases} \ddot{\theta} = \frac{-Mgl_a\cos\theta - D_p\dot{\theta}}{(J_p+Ml_a^2)} - \frac{Ml_a^2\dot{\phi}^2\sin\theta\cos\theta}{(J_p+Ml_a^2)} \\ \qquad + \frac{K_{pp}V_p+K_{py}V_y}{(J_p+Ml_a^2)}, \\ \ddot{\phi} = \frac{-D_y\dot{\phi}}{(J_y+Ml_a^2\cos^2\theta)} + \frac{2Ml_a^2\dot{\phi}\dot{\theta}\sin\theta\cos\theta}{(J_y+Ml_a^2\cos^2\theta)} \\ \qquad + \frac{K_{yp}V_p+K_{yy}V_y}{(J_y+Ml_a^2\cos^2\theta)}, \end{cases} \tag{1}$$

where D_y and D_p are the friction coefficients acting on yaw and pitch axes, l_a represents the distance from the helicopter's center of mass to the origin of the fixed frame, J_p and J_y stand for the moments of inertia, M denotes the helicopter's weight, g means the acceleration of gravity, K_{pp}, K_{py}, K_{yy}, and K_{yp} are

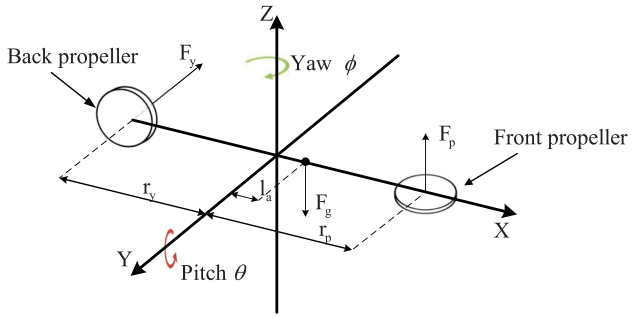

Fig. 1. Diagram of the 2-DOF helicopter model.

the thrust torque constants, ϕ and θ can be indicated as the yaw and pitch angles, respectively. V_p and V_y represent the pitch and yaw motor input voltages, respectively.

Considering the model uncertainty and disturbance existing in the system, the above mathematical model is converted to the following MIMO system by defining $\mathcal{K} = [\mathcal{K}_1, \mathcal{K}_2]^T, \mathcal{K}_1 = [\theta, \phi]^T, \mathcal{K}_2 = [\dot{\theta}, \dot{\phi}]^T$:

$$\begin{cases} \dot{\mathcal{K}}_1 = \mathcal{K}_2, \\ \dot{\mathcal{K}}_2 = A(\mathcal{K}) + \Delta A(\mathcal{K}) + B(\mathcal{K})u + \bar{d} \\ y = \mathcal{K}_1 \end{cases} \tag{2}$$

where $\Delta A(\mathcal{K}) \in R^2$ denotes the model uncertainty, $\bar{d} = [\bar{d}_1, \bar{d}_2]^T$ is external disturbance satisfying $\|\bar{d}\| \le \bar{d}^*$, $\bar{d}^* > 0$ is a unknown constant. $u = [V_p, V_y]^T$ represents the control input. Furthermore, $A(\mathcal{K})$ and $B(\mathcal{K})$ are given by

$$A(\mathcal{K}) = \begin{bmatrix} \frac{-Mgl_a\cos(\mathcal{K}_{11}) - D_p\mathcal{K}_{21} - Ml_a^2\mathcal{K}_{22}^2\sin(\mathcal{K}_{11})\cos(\mathcal{K}_{11})}{J_p + Ml_a^2} \\ \frac{-D_y\mathcal{K}_{22} + 2Ml_a^2\mathcal{K}_{22}\mathcal{K}_{21}\sin(\mathcal{K}_{11})\cos(\mathcal{K}_{11})}{J_y + Ml_a^2\cos^2(\mathcal{K}_{11})} \end{bmatrix}$$

$$B(\mathcal{K}) = \begin{bmatrix} \frac{K_{pp}}{J_p + Ml_a^2} & \frac{K_{py}}{J_p + Ml_a^2} \\ \frac{K_{yp}}{J_y + Ml_a^2\cos^2(\mathcal{K}_{11})} & \frac{K_{yy}}{J_y + Ml_a^2\cos^2(\mathcal{K}_{11})} \end{bmatrix}.$$

Next, a hysteresis quantizer is developed to obtain the quantized control signal while weakening the chattering during the signal quantization, where $u = Q(\tau)$. Based on [35], the quantizer is described as

$$Q(\tau_j) = \begin{cases} \tau_{ji}\text{sig}(\tau_j), & \frac{\tau_{ji}}{1+\delta_j} < |\tau_j| \le \tau_{ji}, \dot{\tau}_j < 0, \text{or} \\ & \tau_{ji} < |\tau_j| \le \frac{\tau_{ji}}{1-\delta_j}, \dot{\tau}_j > 0 \\ \tau_{ji}(1+\delta_j)\text{sig}(\tau_j), & \tau_{ji} < |\tau_j| \le \frac{\tau_{ji}}{1-\delta_j}, \dot{\tau}_j < 0, \text{or} \\ & \frac{\tau_{ji}}{1-\delta_j} < |\tau_j| \le \frac{\tau_{ji}(1+\delta_j)}{1-\delta_j}, \dot{\tau}_j > 0 \\ 0, & 0 \le |\tau_j| < \frac{\tau_{j\min}}{1+\delta_j}, \dot{\tau}_j < 0, \text{or} \\ & \frac{\tau_{j\min}}{1+\delta_j} \le |\tau_j| \le \tau_{j\min}, \dot{\tau}_j > 0 \\ Q(\tau_j(t^-)), & \dot{\tau}_j = 0, j = 1, 2, \end{cases}$$

where $\tau_{ji} = \rho_j^{1-i}\tau_{j\min}, (i = 1, 2, \dots), \delta_j = \frac{1-\rho_j}{1+\rho_j}, \tau_{j\min} > 0$, and $0 < \rho_j < 1$ is the measurement of quantization density. Thus,we can get $Q(\tau_j) \in U = \{0, \pm\tau_{ji}, \pm\tau_{ji}(1+\delta_j)\}$. $\tau_{j\min}$ stands for quantized dead zone size, and $Q(\tau_j(t^-))$ stands for the previous moment of the $Q(\tau_j)$. To facilitate a more intuitive analysis of the quantization effects, we recast the hysteresis quantizer $Q(\tau_j)$ as

$$Q(\tau) = \mathcal{A}\tau(t) + \mathcal{T} \tag{3}$$

where $Q(\tau) = [Q(\tau_1), Q(\tau_2)]^T, \mathcal{A} = \text{diag}\{\mathcal{A}_1, \mathcal{A}_2\}$, and $\mathcal{T} = [\mathcal{T}_1, \mathcal{T}_2]^T$ Then, $\mathcal{A}_j$ and $\mathcal{T}_j$ satisfy the condition $1 - \delta_j \le \mathcal{A}_j \le 1 + \delta_j$, $|\mathcal{T}_j| \le \tau_{j\min}$.

B. Preliminaries

Assumption 1: The desired reference signal is a continuous smooth bounded function when $t > 0$, and its first-order derivative is bounded.

Assumption 2: [36] $B(\mathcal{K})$ is nonsingular, and there exists an unknown positive constant $B^* > 0$ such that the relationship $\|B(\mathcal{K})\| \le B^*$ holds.

Remark 1: Noted that Assumption 1 has been widely adopted in the existing results about adaptive tracking control of nonlinear systems, which is relatively mild and will not pose strict restrictions on actual applications. In addition, Considering that the elements $B_{11} = \frac{K_{pp}}{J_p + Ml_a^2}, B_{12} = \frac{K_{py}}{J_p + Ml_a^2}, B_{21} = \frac{K_{yp}}{J_y + Ml_a^2\cos^2(\mathcal{K}_{11})}$, and $B_{22} = \frac{K_{yy}}{J_y + Ml_a^2\cos^2(\mathcal{K}_{11})}$ of matrix $B(\mathcal{K})$ are bounded, the boundedness of $B(\mathcal{K})$ can be ensured as discussed in [11], [36], and there exists a positive constant $B^* > 0$ such that $\|B(\mathcal{K})\| \le B^*$. Therefore, Assumption 2 is also reasonable.

Lemma 1 [37]: For any constants $\epsilon \ge 0$ and $\vartheta \in R$, one has

$$0 \le |\vartheta| - \frac{\vartheta^2}{\sqrt{\vartheta^2 + \epsilon^2}} \le \epsilon.$$

Lemma 2 [38]: For the continuous smooth function $\mathfrak{F}(\mathfrak{X})$, $R^m \to R$, the radial basis function neural networks (RBFNNs) can be utilized to achieve function approximation satisfying

$$\mathfrak{F}(\mathfrak{X}) = \mathfrak{W}^T H(\mathfrak{X}) \tag{4}$$

where $\mathfrak{X} \in \Omega_{\mathfrak{X}} \subset R^m$ represents the input and $\mathfrak{W} \in R^p$ denotes the weight vector, and $H(\mathfrak{X}) = [H_1(\mathfrak{X}), \dots, H_p(\mathfrak{X})]^T$ stands for the basis function. Furthermore, the unknown continuous smooth function $\mathfrak{F}(\mathfrak{X})$ can be rewritten as follows:

$$\mathfrak{F}(\mathfrak{X}) = \mathfrak{W}^{*T} H(\mathfrak{X}) + \Xi(\mathfrak{X}) \tag{5}$$

where $\mathfrak{W}^*$ denotes the ideal weight vector, Ξ is an approximation error satisfying $\|\Xi(\mathfrak{X})\| \le \Xi^*$, and $\Xi^* > 0$ is a constant. In addition, $\mathfrak{W}^*$ can be defined as follows:

$$\mathfrak{W}^* = \arg\min_{\mathfrak{W} \in R^p} \left\{ \sup_{\mathfrak{X} \in \Omega_{\mathfrak{X}}} \|\mathfrak{F}(\mathfrak{X}) - \mathfrak{W}^T H(\mathfrak{X})\| \right\}. \tag{6}$$

Lemma 3 [39]: For $\mathfrak{C}_1 \in \mathbb{R}$ and $\mathfrak{C}_2 \in \mathbb{R}$, it has

$$|\mathfrak{C}_1|^{\mathcal{N}_1}|\mathfrak{C}_2|^{\mathcal{N}_2} \le \frac{\mathcal{N}_1\iota}{\mathcal{N}_1 + \mathcal{N}_2}|\mathfrak{C}_1|^{\mathcal{N}_1 + \mathcal{N}_2} + \frac{\mathcal{N}_2\iota^{\frac{-\mathcal{N}_1}{\mathcal{N}_2}}}{\mathcal{N}_1 + \mathcal{N}_2}|\mathfrak{C}_2|^{\mathcal{N}_1 + \mathcal{N}_2}$$

where $\mathcal{N}_1 > 0, \mathcal{N}_2 > 0$, and $\iota > 0$.

Lemma 4 [40]: For $x_i \ge 0, i \in N^+$ and $a > 0$, the following relationships hold

$$\begin{cases} \sum_{i=1}^n x_i^a \ge (\sum_{i=1}^n x_i)^a, & \text{if } 0 < a < 1 \\ \sum_{i=1}^n x_i^a \ge n^{1-a}(\sum_{i=1}^n x_i)^a, & \text{if } a > 1. \end{cases} \tag{7}$$

Lemma 5 [41]: For the system $\dot{\mathcal{X}} = f(t, \mathcal{X})$. If the continuous function $V(\mathcal{X})$ fulfills the following inequality:

$$\dot{V} \leq -\frac{\pi}{\gamma T_c \sqrt{\beta_1 \beta_2}}(\beta_1 V^{(2-\gamma)/2} + \beta_2 V^{(2+\gamma)/2}) + \mathfrak{d} \quad (8)$$

where $0 < \gamma < 1$, $0 < \mathfrak{d} < \infty$, $T_c > 0$, β_1 and β_2 are positive constants, the investigated system is called practical predefined-time stable (PPTS). Furthermore, the residual set of the system can be described by

$$\left\{ \lim_{t \to T_p} \mathcal{X} \mid V \leq \min \left\{ \left(\frac{2\gamma T_c \varrho \sqrt{\beta_1 \beta_2}}{\pi \beta_1} \right)^{\frac{2}{2-\gamma}}, \left(\frac{2\gamma T_c \varrho \sqrt{\beta_1 \beta_2}}{\pi \beta_2} \right)^{\frac{2}{2+\gamma}} \right\} \right\}$$

where T_p denotes the upper bound of the minimum settling time and $T_p < T_{max} = \sqrt{2} T_c$.

This work aims to devise a predefined-time neural adaptive quantized self-triggered control (STC) design with appointed performance for a 2-DOFHS such that all signals in the closed-loop system (CLS) are PPTB, and the tracking error can be effectively regulated into the neighborhood of the origin satisfying a preassigned transient and steady-state performance.

III. Main Result

A. Predefined-Time Self-Triggered Quantized Control Design With Appointed Tracking Performance

First, we define an error variable e_1 as

$$e_1 = \mathcal{K}_1 - \mathcal{K}_d \quad (9)$$

where $\mathcal{K}_d$ is the desired trajectory. In order to obtain better transient performance, we impose the following constraints on the tracking error:

$$-\underline{\eta}_i \psi_i(t) < e_{1,i}(t) < \overline{\eta}_i \psi_i(t), (i = 1, 2) \quad (10)$$

where $\underline{\eta}_i > 0$ and $\overline{\eta}_i > 0$ stand for set parameters, $\psi_i(t)$ represents the performance function satisfying

$$\psi_i(t) = \begin{cases} (\psi_{i0} - \overline{\psi}_i) e^{(-\varpi_i t)} \left(1 - \frac{t}{T_i}\right)^{\frac{1}{1-\zeta_i}} + \overline{\psi}_i, 0 \leq t \leq T_i \\ \overline{\psi}_i, \qquad t > T_i \end{cases} \quad (11)$$

where $T_i > 0$ indicates the preset time, $\varpi_i > 0, \zeta_i \in (1/2, 1), \psi_i(0) = \psi_{i0}, \psi_i(T_i) = \overline{\psi}_i, \psi_{i0} > 0$ and $\overline{\psi}_i > 0$ denote constants, $\psi_{i0} > \overline{\psi}_i$.

Asymmetric constraint (10) is converted to the following symmetric constraint:

$$-p_i(t) < \mathfrak{B}_i(t) < p_i(t) \quad (12)$$

where $\mathfrak{B}_i(t) = e_{1,i}(t)/\psi_i(t) + 1/2(\underline{\eta}_i - \overline{\eta}_i), p_i(t) = 1/2(\underline{\eta}_i + \overline{\eta}_i)$.

The error transformation is defined as

$$\mathfrak{B}_i(t) = p_i(t) \mathfrak{f}_i(\varepsilon_i(t)) \quad (13)$$

where $\mathfrak{f}_i(\varepsilon_i(t))$ denotes a smooth function of the strictly monotonically increasing and satisfies the following conditions:

$$\begin{cases} \lim_{(\varepsilon_i(t)) \to -\infty} \mathfrak{f}_i(\varepsilon_i(t)) = -1 \\ \lim_{(\varepsilon_i(t)) \to +\infty} \mathfrak{f}_i(\varepsilon_i(t)) = 1. \end{cases} \quad (14)$$

Based on the above conditions, we define the following transformation function:

$$\mathfrak{f}_i(\varepsilon_i(t)) = \frac{2}{\pi} \arctan(\varepsilon_i(t)). \quad (15)$$

According to (13) and (15), the unconstrained transformation error can be represented as

$$\varepsilon_i(t) = \tan\left(\frac{\pi \mathfrak{B}_i(t)}{2 p_i(t)}\right) \quad (16)$$

with $\mathfrak{B}_i(0) < p_i(0)$.

Then, the derivative of $\mathfrak{B}_i(t)$ is

$$\dot{\mathfrak{B}}_i(t) = \frac{2}{\pi} p_i(t) \frac{\dot{\varepsilon}_i(t)}{1 + \varepsilon_i^2(t)} = \frac{\dot{e}_{1,i}(t)}{\psi_i(t)} - \frac{e_{1,i}(t) \dot{\psi}_i(t)}{\psi_i^2(t)}. \quad (17)$$

Furthermore, we have

$$\dot{\varepsilon}_i(t) = d_{1,i}(t) \left(\dot{e}_{1,i}(t) - \frac{e_{1,i}(t) \dot{\psi}_i(t)}{\psi_i(t)} \right) \quad (18)$$

where $d_{1,i}(t) = \frac{\pi(1+\varepsilon_i^2(t))}{(2 p_i(t) \psi_i(t))}$ is a known positive function.

Given attention to both the problem of "complexity explosion" exposed in traditional backstepping design and convergence property of filter error existing in DSC method, a novel PT filter is given as

$$\xi \dot{\alpha}_f = -w_1 \mathrm{sig}^{1-\gamma}(s) - w_2 \mathrm{sig}^{1+\gamma}(s) - \frac{1}{2} s - \frac{\xi \hat{\sigma}^2 s}{\sqrt{(s^T s)\hat{\sigma}^2 + \bar{\Delta}^2}} \quad (19)$$

where $\alpha_f(0) = \alpha(0)$, α_f represents a variable of newly introduced, $s = \alpha_f - \alpha$ stands for the filter error, w_1, w_2 and ξ are positive constants, satisfying $w_1 = \frac{\pi \beta_1}{\gamma T_c \sqrt{\beta_1 \beta_2}} (\frac{2}{\xi})^{1-\gamma/2}$ and $w_2 = \frac{\pi \beta_2}{\gamma T_c \sqrt{\beta_1 \beta_2}} 3^{\frac{3\gamma}{2}} 2^{\frac{\gamma}{2}} (\frac{2}{\xi})^{1+\gamma/2}$, respectively. $\bar{\Delta}$ is a positive time-varying parameter.

For the continuous function α, there exist an unknown positive constant σ such that inequality $\|\dot{\alpha}\| \leq \sigma$ holds. The estimation error is defined as $\tilde{\sigma} = \sigma - \hat{\sigma}$. $\hat{\sigma}$ denotes the estimation of parameter σ, which is determined by

$$\dot{\hat{\sigma}} = \xi \|s\| - h \hat{\sigma} - b_1 \hat{\sigma}^{1+\gamma} \quad (20)$$

where $h = (\frac{\pi \beta_1}{\gamma T_c \sqrt{\beta_1 \beta_2}})^{\frac{2}{2-\gamma}}$, and $b_1 = \frac{\pi \beta_2}{\gamma T_c \sqrt{\beta_1 \beta_2}} \frac{(2+\gamma) 3^{\frac{3\gamma}{2}}}{2^{1+\frac{\gamma}{2}}(1+\gamma)}$.

Remark 2: In some existing DSC results, the first-order filter $\xi \dot{\alpha}_f + \alpha_f = \alpha$ with $\alpha_f = 0$ has been widely adopted to evade the issue of the computational complexity. Unfortunately, the convergence characteristic of the filter error has not been paid enough attention in the above-mentioned results. To this end, a novel nonlinear filter (19) associated with parameter update law (20) is constructed in the procedure of recursive design in this

work, which not only can avoid the issue of "explosion of complexity", but also can ensure the predefined-time convergence of filter error.

By defining $\varepsilon = [\varepsilon_1, \varepsilon_2]^T$, the coordinate transformation is given by

$$\begin{cases} z_1 = \varepsilon \\ z_2 = \mathcal{K}_2 - \alpha_f. \end{cases} \tag{21}$$

Step 1*:* Select the following Lyapunov function:

$$V_1 = \frac{1}{2} z_1^T \mathcal{D}^{-1} z_1 + \frac{\xi}{2} s^T s + \frac{1}{2}\tilde{\sigma}^2 \tag{22}$$

where $\mathcal{D} = \mathrm{diag}\{d_{1,1}, d_{1,2}\}$.

The derivative of V_1 is

$$\begin{aligned} \dot{V}_1 = {} & z_1^T (z_2 + s + \alpha - \dot{\mathcal{K}}_d - \mathfrak{D}_1) \\ & + s^T \xi (\dot{\alpha}_f - \dot{\alpha}) - \tilde{\sigma}\dot{\hat{\sigma}}. \end{aligned} \tag{23}$$

The virtual controller $\alpha = [\alpha_1, \alpha_2]^T$ is proposed as

$$\alpha = -\frac{z_1 \bar{\alpha}^T \bar{\alpha}}{\sqrt{z_1^T z_1 \bar{\alpha}^T \bar{\alpha} + \epsilon_1^2}} + \dot{\mathcal{K}}_d + \mathfrak{D}_1 \tag{24}$$

$$\begin{aligned} \bar{\alpha} = {} & \mathfrak{b}_1 z_1 + \frac{\pi}{\gamma T_c \sqrt{\beta_1 \beta_2}} \Bigg[\beta_1 \left(\frac{1}{2} \mathcal{D}^{-1} \right)^{1-\frac{\gamma}{2}} \cdot \mathrm{sig}^{1-\gamma}(z_1) \\ & + 3^{\frac{3\gamma}{2}} 2^{\frac{\gamma}{2}} \beta_2 \left(\frac{1}{2} \mathcal{D}^{-1} \right)^{1+\frac{\gamma}{2}} \cdot \mathrm{sig}^{1+\gamma}(z_1) \Bigg] \end{aligned} \tag{25}$$

where $\mathfrak{D}_1 = [\frac{e_{1,1}(t)\dot{\psi}_1(t)}{\psi_1(t)}, \frac{e_{1,2}(t)\dot{\psi}_2(t)}{\psi_2(t)}]^T, \epsilon_1 > 0, \mathfrak{b}_1 \geq 1$ and T_c stands for a predefined constant.

Then substituting (24) and (25) into (23) and using Lemmas 1 and 4, (23) becomes

$$\begin{aligned} \dot{V}_1 \leq {} & -\frac{\pi\beta_1}{\gamma T_c \sqrt{\beta_1\beta_2}} \left(\frac{1}{2}\mathcal{Z}_1 \right)^{1-\frac{\gamma}{2}} + \frac{\|z_2\|^2}{2} + \frac{\|s\|^2}{2} \\ & - \frac{\pi\beta_2}{\gamma T_c \sqrt{\beta_1\beta_2}} 3^{\frac{3\gamma}{2}} \left(\frac{1}{2}\mathcal{Z}_1 \right)^{1+\frac{\gamma}{2}} + s^T \xi (\dot{\alpha}_f - \dot{\alpha}) \\ & + \epsilon_1 - \tilde{\sigma}\dot{\hat{\sigma}} \end{aligned} \tag{26}$$

where $\mathcal{Z}_1 = z_1^T \mathcal{D}^{-1} z_1$.

Substituting (19) and (20) into (26) results in

$$\begin{aligned} \dot{V}_1 \leq {} & \frac{1}{2}\|z_2\|^2 - w_1 \|s\|^{2-\gamma} - w_2 \|s\|^{2+\gamma} \\ & - \frac{\pi\beta_1}{\gamma T_c \sqrt{\beta_1\beta_2}} \left(\frac{1}{2}\mathcal{Z}_1 \right)^{1-\frac{\gamma}{2}} \\ & - \frac{\pi\beta_2}{\gamma T_c \sqrt{\beta_1\beta_2}} 3^{\frac{3\gamma}{2}} \left(\frac{1}{2}\mathcal{Z}_1 \right)^{1+\frac{\gamma}{2}} \\ & + h\tilde{\sigma}\hat{\sigma} + b_1 \tilde{\sigma}\hat{\sigma}^{1+\gamma} + \xi\bar{\Delta} + \epsilon_1. \end{aligned} \tag{27}$$

Utilizing the Young's inequality, one can obtain

$$h\tilde{\sigma}\hat{\sigma} \leq -\frac{h\tilde{\sigma}^2}{2} + \frac{h\sigma^2}{2}. \tag{28}$$

Substituting (28) into (27) yields

$$\begin{aligned} \dot{V}_1 \leq {} & \frac{1}{2}\|z_2\|^2 - w_1 \|s\|^{2-\gamma} - w_2 \|s\|^{2+\gamma} \\ & - \frac{\pi\beta_1}{\gamma T_c \sqrt{\beta_1\beta_2}} \left(\frac{1}{2}\mathcal{Z}_1 \right)^{1-\frac{\gamma}{2}} \\ & - \frac{\pi\beta_2}{\gamma T_c \sqrt{\beta_1\beta_2}} 3^{\frac{3\gamma}{2}} \left(\frac{1}{2}\mathcal{Z}_1 \right)^{1+\frac{\gamma}{2}} \\ & - \frac{h\tilde{\sigma}^2}{2} + \frac{h\sigma^2}{2} + b_1 \tilde{\sigma}\hat{\sigma}^{1+\gamma} + \xi\bar{\Delta} + \epsilon_1. \end{aligned} \tag{29}$$

Based on Lemma 3, we have

$$\left(\frac{h\tilde{\sigma}^2}{2} \right)^{1-\frac{\gamma}{2}} \leq \mathfrak{A}_1(\gamma) + \frac{h\tilde{\sigma}^2}{2} \tag{30}$$

where $\mathfrak{A}_1(\gamma) = \frac{\gamma}{2}(1-\frac{\gamma}{2})^{\frac{2-\gamma}{\gamma}}$.

According to [42], one yields $x(y-x)^\nu \leq \frac{\nu}{1+\nu}(y^{1+\nu} - x^{1+\nu})$ for $y \geq x$ and $\nu > 1$. Similarly, one can obtain

$$\tilde{\sigma}\hat{\sigma}^{1+\gamma} \leq \frac{1+\gamma}{2+\gamma} \left(\sigma^{2+\gamma} - \tilde{\sigma}^{2+\gamma} \right). \tag{31}$$

Substituting (30) and (31) into (29) yields

$$\begin{aligned} \dot{V}_1 \leq {} & \frac{1}{2}\|z_2\|^2 - w_1 \|s\|^{2-\gamma} - w_2 \|s\|^{2+\gamma} \\ & - \frac{\pi\beta_1}{\gamma T_c \sqrt{\beta_1\beta_2}} \left(\frac{1}{2}\mathcal{Z}_1 \right)^{1-\frac{\gamma}{2}} + \frac{h\sigma^2}{2} + b_1 \frac{1+\gamma}{2+\gamma}\sigma^{2+\gamma} \\ & - \frac{\pi\beta_2}{\gamma T_c \sqrt{\beta_1\beta_2}} 3^{\frac{3\gamma}{2}} \left(\frac{1}{2}\mathcal{Z}_1 \right)^{1+\frac{\gamma}{2}} - \left(\frac{h\tilde{\sigma}^2}{2} \right)^{1-\frac{\gamma}{2}} \\ & - \frac{2^{1+\frac{\gamma}{2}} b_1 (1+\gamma)}{2+\gamma} \left(\frac{\tilde{\sigma}^2}{2} \right)^{1+\frac{\gamma}{2}} + \epsilon_1 + \mathfrak{A}_1(\gamma) \\ \leq {} & -\frac{\pi\beta_1 V_1^{1-\frac{\gamma}{2}}}{\gamma T_c \sqrt{\beta_1\beta_2}} - \frac{3^\gamma \pi\beta_2 V_1^{1+\frac{\gamma}{2}}}{\gamma T_c \sqrt{\beta_1\beta_2}} + \frac{\|z_2\|^2}{2} + \mathfrak{a}_1 \end{aligned} \tag{32}$$

where $\mathfrak{a}_1 = \xi\bar{\Delta} + \epsilon_1 + \mathfrak{A}_1(\gamma) + \frac{h\sigma^2}{2} + b_1 \frac{1+\gamma}{2+\gamma}\sigma^{2+\gamma}$.

Step 2*:* To reduce the control signal update frequency and avoid the continuous monitoring of the event-triggered mechanisms, the following self-triggered mechanism is introduced to release communication burden in this step:

$$\tau_i(t) = \mu_i(t_q^i), \quad \forall t \in \left[t_q^i, t_{q+1}^i \right), \quad i = 1, 2. \tag{33}$$

$$t_{q+1}^i = t_q^i + \frac{c_i |\tau_i(t)| + n_i}{\max\{|\dot{\mu}_i(t)|, m_i\}}, \tag{34}$$

where μ_i denotes the control input signal and will be designed later. $c_i|\tau_i(t)| + n_i$ denote the control signal update interval of previous and next instances. $t_q^i, t_{q+1}^i \in Z^+, 0 < c_i < 1, m_i > 0, n_i > 0$ are the design parameters.

For time-varying continuous functions $|\varphi_{1i}(t)| \leq 1$ and $|\varphi_{2i}(t)| \leq 1$, one has $\varphi_{1i}(t_{q+1}^i) = \varphi_{2i}(t_{q+1}^i) = \pm 1$ and $\varphi_{1i}(t_q^i) = \varphi_{2i}(t_q^i) = 0$. Then, we can further obtain from (33)–(34) that

$$\tau_i(t) = \frac{\mu_i(t) - \varphi_{2i}(t) n_i}{1 + \varphi_{1i}(t) c_i} \tag{35}$$

for time interval $[t_q^i, t_{q+1}^i)$.

Based on formula (35), one can obtain

$$\tau(t) = \mathcal{F}\mu + N \tag{36}$$

where $\mu = [\mu_1, \mu_2]^T, \mathcal{F} = \text{diag}\{\frac{1}{1+\varphi_{11}c_1}, \frac{1}{1+\varphi_{12}c_2}\}$, and $N = [\frac{\varphi_{21}n_1}{1+\varphi_{11}c_1}, \frac{\varphi_{22}n_2}{1+\varphi_{12}c_2}]^T$.

Remark 3: According to the definition in the self-triggered mechanism, $0 < c_i < 1, n_i > 0, |\varphi_{1i}(t)| \leq 1, |\varphi_{2i}(t)| \leq 1$. Then we can get $\frac{1}{1+c_i} \leq \frac{1}{1+\varphi_{1i}c_i} \leq \frac{1}{1-c_i}$ and $\frac{\varphi_{2i}n_i}{1+\varphi_{1i}c_i}$ are bounded. So, we can get the $\mathcal{F}$ and N are bounded.

Considering (3) and (36), we have

$$u(t) = L\mu + M \tag{37}$$

where $L = \mathcal{A}\mathcal{F} = \text{diag}\{\frac{\mathcal{A}_1}{1+\varphi_{11}c_1}, \frac{\mathcal{A}_2}{1+\varphi_{12}c_2}\} = \text{diag}\{l_1, l_2\}$ with $l_i > 0 (i = 1, 2)$ is bounded, so we have $l_0 = \inf_{t\geq 0} \lambda_{\min}(L)$ and $\varrho = [\varrho_1, \varrho_2]^T = [\frac{1}{l_0}, \frac{1}{l_0}]^T$. $M = \mathcal{T} + \mathcal{A}N = [m_1, m_2]^T$.

Further, we redefined the $\dot{\mathcal{K}}_2$ as

$$\dot{\mathcal{K}}_2 = A(\mathcal{K}) + \Delta A(\mathcal{K}) + B(\mathcal{K})L\mu + \mathfrak{M} + \bar{d} \tag{38}$$

where $\mathfrak{M} = B(\mathcal{K})M$.

Then, invoking (21) and (38) gets

$$\dot{z}_2 = A(\mathcal{K}) + \Delta A(\mathcal{K}) + \bar{d} + B(\mathcal{K})L\mu + \mathfrak{M} - \dot{\alpha}_f. \tag{39}$$

Next, the Lyapunov function is selected as

$$V_2 = V_1 + \frac{1}{2}z_2^T z_2 + \frac{l_0}{2\lambda_1}\tilde{\varrho}^2 \tag{40}$$

where $\lambda_1 > 0$, and $\tilde{\varrho} = \varrho - \hat{\varrho}$ is the estimation error.

According to Assumption 2, one gets $\|\mathfrak{M}\| = \|B(\mathcal{K})M\| \leq \mathfrak{M}^*$, where $\mathfrak{M}^*$ denotes a positive constant but unknown. By invoking (38), (21), and (32), the derivative of V_2 is

$$\begin{aligned}\dot{V}_2 \leq & -\frac{\pi\beta_1}{\gamma T_c\sqrt{\beta_1\beta_2}}V_1^{1-\frac{\gamma}{2}} - \frac{\pi\beta_2}{\gamma T_c\sqrt{\beta_1\beta_2}}3^\gamma V_1^{1+\frac{\gamma}{2}} \\ & + \frac{1}{2}\|z_2\|^2 + \mathfrak{a}_1 + z_2^T\left[(A(\mathcal{K}) + \mathfrak{F} + B(\mathcal{K})L\mu\right. \\ & \left. + \mathfrak{M} + \bar{d} - \dot{\alpha}_f\right] - \frac{l_0}{\lambda_1}\tilde{\varrho}\dot{\hat{\varrho}}\end{aligned} \tag{41}$$

in which $\mathfrak{F} = [\mathfrak{F}_1, \mathfrak{F}_2]^T = \Delta A(\mathcal{K})$ is the lumped uncertainty. Using the RBFNN approximation, one can obtain

$$\mathfrak{F} = \mathfrak{W}^{*T}H(\mathfrak{X}) + \Xi(\mathfrak{X}) \tag{42}$$

where $\mathfrak{W}^*$ denotes the ideal weight vector. $H(\mathfrak{X})$ stands for the basis function with $\mathfrak{X} = [\mathcal{K}_1^T, \mathcal{K}_2^T, \mathcal{K}_d^T, \dot{\mathcal{K}}_d^T]^T$, $\Xi(X)$ denotes the approximation error satisfying $\|\Xi\| \leq \Xi^*$.

The predefined-time controller μ is designed as

$$\mu = -B^{-1}(\mathcal{K})\frac{\hat{\varrho}^2 z_2\bar{\mu}^T\bar{\mu}}{\sqrt{\hat{\varrho}^2 z_2^T z_2\bar{\mu}^T\bar{\mu} + \epsilon_2^2}} \tag{43}$$

with

$$\begin{aligned}\bar{\mu} = & \mathfrak{b}_2 z_2 + \frac{\pi}{\gamma T_c\sqrt{\beta_1\beta_2}}\left[\beta_1\left(\frac{1}{2}\right)^{1-\frac{\gamma}{2}}\cdot \text{sig}^{1-\gamma}(z_2)\right. \\ & \left. + 3^\gamma\beta_2\left(\frac{1}{2}\right)^{1+\frac{\gamma}{2}}\cdot \text{sig}^{1+\gamma}(z_2)\right] + A(\mathcal{K}) + \frac{\hat{\upsilon}\chi z_2}{2\mathfrak{c}^2} \\ & + \tanh\left(\frac{z_2}{\mathfrak{e}}\right)\hat{\mathfrak{M}} - \dot{\alpha}_f\end{aligned} \tag{44}$$

where $\chi = \text{diag}\{H_1^T H_1, H_2^T H_2\}, \epsilon_2 \geq 0, \mathfrak{b}_2 \geq 3/2, \mathfrak{c} > 0, \upsilon = \max\{\|\mathfrak{W}_1^*\|^2, \|\mathfrak{W}_2^*\|^2\}$. In addition, $\hat{\upsilon}$ is the estimation of υ and $\tilde{\upsilon} = \upsilon - \hat{\upsilon}$.

Correspondingly, the adaptive law is proposed by

$$\dot{\hat{\varrho}} = \lambda_1 z_2^T\bar{\mu} - h\hat{\varrho} - b_2\hat{\varrho}^{1+\frac{\gamma}{2}} \tag{45}$$

where $b_2 = (\frac{\pi\beta_2 3^\gamma}{\gamma T_c\sqrt{\beta_1\beta_2}})^{\frac{2}{2+\gamma}}$.

Considering the inequality $z_2^T\mathfrak{M} \leq \mathfrak{M}^*\sum_{i=1}^2|z_{2i}|$, we have $z_2^T\tanh(\frac{z_2}{\mathfrak{e}}) = \sum_{i=1}^2(z_{2i}\tanh(\frac{z_{2i}}{\mathfrak{e}}))$. According to [43], one has $0 \leq |c| - c\tanh(c/\mathfrak{e}) \leq 0.2785\mathfrak{e}$ for any $c \in R$ and $\mathfrak{e} > 0$. Then, the following relationship holds:

$$\sum_{i=1}^2|z_{2i}| - \sum_{i=1}^2\left(z_{2i}\tanh\left(\frac{z_{2i}}{\mathfrak{e}}\right)\right) \leq 0.557\mathfrak{e}. \tag{46}$$

Furthermore, the parameter update laws $\dot{\hat{\upsilon}}$ and $\dot{\hat{\mathfrak{M}}}$ are constructed with the following forms:

$$\dot{\hat{\upsilon}} = \frac{1}{2\mathfrak{c}^2}\sum_{i=1}^2 z_{2i}^2 H_i^T H_i - h\hat{\upsilon} - b_3\hat{\upsilon}^{1+\gamma} \tag{47}$$

$$\dot{\hat{\mathfrak{M}}} = \lambda_2 z_2^T\tanh\left(\frac{z_2}{\mathfrak{e}}\right) - h\hat{\mathfrak{M}} - b_4\hat{\mathfrak{M}}^{1+\gamma} \tag{48}$$

where $h = (\frac{\pi\beta_1}{\gamma T_c\sqrt{\beta_1\beta_2}})^{\frac{2}{2-\gamma}}$, $b_3 = \frac{\pi\beta_2}{\gamma T_c\sqrt{\beta_1\beta_2}}\frac{(2+\gamma)3^{\frac{\gamma}{2}}}{2^{1+\frac{\gamma}{2}}(1+\gamma)}$ and $b_4 = \frac{\pi\beta_2}{\gamma T_c\sqrt{\beta_1\beta_2}}\frac{(2+\gamma)3^{\frac{\gamma}{2}}}{2^{1+\frac{\gamma}{2}}\lambda_2^{\frac{\gamma}{2}}(1+\gamma)}$. $\hat{\mathfrak{M}}$ stands for the estimation of $\mathfrak{M}^*$ and satisfies $\tilde{\mathfrak{M}} = \mathfrak{M}^* - \hat{\mathfrak{M}}$.

Substituting (43) and (45) into (41) yields

$$\begin{aligned}\dot{V}_2 \leq & -\frac{\pi\beta_1}{\gamma T_c\sqrt{\beta_1\beta_2}}V_1^{1-\frac{\gamma}{2}} - \frac{\pi\beta_2}{\gamma T_c\sqrt{\beta_1\beta_2}}3^\gamma V_1^{1+\frac{\gamma}{2}} \\ & + \frac{1}{2}\|z_2\|^2 + \mathfrak{a}_1 + z_2^T\mathfrak{F} + z_2^T A(\mathcal{K}) + l_0\epsilon_2 \\ & - z_2^T\bar{\mu} + \frac{l_0 h}{\lambda_1}\tilde{\varrho}\hat{\varrho} + \frac{l_0 b_2}{\lambda_1}\tilde{\varrho}\hat{\varrho}^{1+\frac{\gamma}{2}} + z_2^T\bar{d}.\end{aligned} \tag{49}$$

Utilizing the Young's inequality, one has

$$z_2^T\mathfrak{F} \leq \frac{\upsilon}{2\mathfrak{c}^2}\sum_{i=1}^2 z_{2i}^2 H_i^T H_i + \mathfrak{c}^2 + \frac{\|z_2\|^2}{2} + \Xi^{*2} \tag{50}$$

$$z_2^T\bar{d} \leq \frac{1}{2}\|z_2\|^2 + \frac{1}{2}\bar{d}^{*2} \tag{51}$$

$$\frac{l_0 h}{\lambda_1}\tilde{\varrho}\hat{\varrho} \leq -\frac{l_0 h}{2\lambda_1}\tilde{\varrho}^2 + \frac{l_0 h}{2\lambda_1}\varrho^2. \tag{52}$$

According to Lemma 3, we have

$$\begin{aligned}\frac{l_0 b_2}{\lambda_1}\tilde{\varrho}\hat{\varrho}^{1+\frac{\gamma}{2}} \leq & \left(\frac{l_0 b_2}{\lambda_1}\right)^{1+\frac{\gamma}{2}}\left(\frac{\varrho^2}{2}\right)^{1+\frac{\gamma}{2}} \\ & - \left(\frac{l_0 b_2}{\lambda_1}\right)^{1+\frac{\gamma}{2}}\left(\frac{\tilde{\varrho}^2}{2}\right)^{1+\frac{\gamma}{2}} + \mathfrak{A}_2(\gamma)\hat{\varrho}^{1+\frac{\gamma}{2}}\end{aligned} \tag{53}$$

where $\mathfrak{A}_2(\gamma) = \frac{\gamma}{2+\gamma}(\frac{2}{2+\gamma})^{\frac{2}{\gamma}}$.

Substituting (44), (50)–(53) into (49) yields

$$\begin{aligned}\dot{V}_2 \leq & -\frac{\pi\beta_1}{\gamma T_c\sqrt{\beta_1\beta_2}}V_1^{1-\frac{\gamma}{2}}-\frac{\pi\beta_2}{\gamma T_c\sqrt{\beta_1\beta_2}}3^{\gamma}V_1^{1+\frac{\gamma}{2}}+\mathfrak{a}_1\\&+\frac{\tilde{\upsilon}}{2\mathfrak{e}^2}\sum_{i=1}^{2}z_{2i}^2H_i^TH_i+\Xi^{*2}+l_0\epsilon_2-\frac{l_0h}{2\lambda_1}\tilde{\varrho}^2+\frac{l_0h}{2\lambda_1}\varrho^2\\&-\frac{\pi\beta_1}{\gamma T_c\sqrt{\beta_1\beta_2}}\left(\frac{\|z_2\|^2}{2}\right)^{1-\frac{\gamma}{2}}+\left(\frac{l_0b_2}{\lambda_1}\right)^{1+\frac{\gamma}{2}}\left(\frac{\varrho^2}{2}\right)^{1+\frac{\gamma}{2}}\\&-\frac{\pi\beta_2 3^{\gamma}}{\gamma T_c\sqrt{\beta_1\beta_2}}\left(\frac{\|z_2\|^2}{2}\right)^{1+\frac{\gamma}{2}}-\left(\frac{l_0b_2}{\lambda_1}\right)^{1+\frac{\gamma}{2}}\left(\frac{\tilde{\varrho}^2}{2}\right)^{1+\frac{\gamma}{2}}\\&+\mathfrak{A}_2(\gamma)\hat{\varrho}^{1+\frac{\gamma}{2}}+\mathfrak{e}^2+z_2^T\tanh\left(\frac{z_2}{\mathfrak{e}}\right)\mathfrak{M}\\&+0.557\mathfrak{e}\mathfrak{M}^*+\frac{1}{2}\bar{d}^{*2}.\end{aligned}\tag{54}$$

Based on Lemma 3, we have

$$\left(\frac{l_0h}{2\lambda_1}\tilde{\varrho}^2\right)^{1-\frac{\gamma}{2}}\leq\mathfrak{A}_3(\gamma)+\frac{l_0h}{2\lambda_1}\tilde{\varrho}^2\tag{55}$$

where $\mathfrak{A}_3(\gamma)=\frac{\gamma}{2}(1-\frac{\gamma}{2})^{\frac{2-\gamma}{\gamma}}$.

Substituting (55) into (54) yields

$$\begin{aligned}\dot{V}_2\leq & -\frac{\pi\beta_1}{\gamma T_c\sqrt{\beta_1\beta_2}}V_2^{1-\frac{\gamma}{2}}-\frac{\pi\beta_2}{\gamma T_c\sqrt{\beta_1\beta_2}}3^{\frac{\gamma}{2}}V_2^{1+\frac{\gamma}{2}}\\&+\frac{\tilde{\upsilon}}{2\mathfrak{e}^2}\sum_{i=1}^{2}z_{2i}^2H_i^TH_i+z_2^T\tanh\left(\frac{z_2}{\mathfrak{e}}\right)\mathfrak{M}+\mathfrak{a}_2\end{aligned}\tag{56}$$

where $\mathfrak{a}_2=\mathfrak{a}_1+\mathfrak{e}^2+\Xi^{*2}+l_0\epsilon_2+\frac{l_0h}{2\lambda_1}\varrho^2+\mathfrak{A}_2(\gamma)\hat{\varrho}^{1+\frac{\gamma}{2}}+\mathfrak{A}_3(\gamma)+(\frac{l_0b_2}{\lambda_1})^{1+\frac{\gamma}{2}}(\frac{1}{2}\varrho^2)^{1+\frac{\gamma}{2}}+0.557\mathfrak{e}\mathfrak{M}^*+\frac{1}{2}\bar{d}^{*2}$.

B. Stability Analysis

Theorem 1. Consider the 2-DOF helicopter system described by (1) under Assumptions 1-2, if the proposed control scheme including the PT filter (19), virtual controller (24), PT controller (43), and parameter update laws (20), (45), (44) are adopted, the following points can be ensured:

All signals in the CLS are PPTB;

The tracking errors can be regulated into a preassigned area within a predefined time satisfying an appointed tracking performance;

The Zeno behavior can be excluded.

Proof:

Select the Lyapunov function as:

$$V_3=V_2+\frac{1}{2}\tilde{\upsilon}^2+\frac{1}{2\lambda_2}\tilde{\mathfrak{M}}^2\tag{57}$$

Differentiating (57) yields

$$\begin{aligned}\dot{V}_3\leq & -\frac{\pi\beta_1}{\gamma T_c\sqrt{\beta_1\beta_2}}V_2^{1-\frac{\gamma}{2}}-\frac{\pi\beta_2}{\gamma T_c\sqrt{\beta_1\beta_2}}3^{\frac{\gamma}{2}}V_2^{1+\frac{\gamma}{2}}\\&+\tilde{\upsilon}\left(\frac{1}{2\mathfrak{e}^2}\sum_{i=1}^{2}z_{2i}^2H_i^TH_i-\dot{\hat{\upsilon}}\right)-\frac{1}{\lambda_2}\tilde{\mathfrak{M}}\dot{\hat{\mathfrak{M}}}\\&+z_2^T\tanh\left(\frac{z_2}{\mathfrak{e}}\right)\tilde{\mathfrak{M}}+\mathfrak{a}_2.\end{aligned}\tag{58}$$

Substituting (47) and (48) into (58) yields

$$\begin{aligned}\dot{V}_3\leq & -\frac{\pi\beta_1}{\gamma T_c\sqrt{\beta_1\beta_2}}V_2^{1-\frac{\gamma}{2}}-\frac{\pi\beta_2}{\gamma T_c\sqrt{\beta_1\beta_2}}2^{\frac{\gamma}{2}}V_2^{1+\frac{\gamma}{2}}+h\tilde{\upsilon}\hat{\upsilon}\\&+b_3\tilde{\upsilon}\hat{\upsilon}^{1+\gamma}+\mathfrak{a}_2+\frac{h}{\lambda_2}\tilde{\mathfrak{M}}\hat{\mathfrak{M}}+\frac{b_4}{\lambda_2}\tilde{\mathfrak{M}}\hat{\mathfrak{M}}^{1+\gamma}.\end{aligned}\tag{59}$$

Utilizing the Young's inequality gets

$$h\tilde{\upsilon}\hat{\upsilon}\leq-\frac{h\tilde{\upsilon}^2}{2}+\frac{h\upsilon^2}{2}\tag{60}$$

$$\frac{h}{\lambda_2}\tilde{\mathfrak{M}}\hat{\mathfrak{M}}\leq-\frac{h\tilde{\mathfrak{M}}^2}{2\lambda_2}+\frac{h\mathfrak{M}^{*2}}{2\lambda_2}.\tag{61}$$

Invoking (59) and (60), one has

$$\begin{aligned}\dot{V}_3\leq & -\frac{\pi\beta_1}{\gamma T_c\sqrt{\beta_1\beta_2}}V_2^{1-\frac{\gamma}{2}}-\frac{\pi\beta_2}{\gamma T_c\sqrt{\beta_1\beta_2}}2^{\frac{\gamma}{2}}V_2^{1+\frac{\gamma}{2}}\\&-\frac{h\tilde{\upsilon}^2}{2}+\frac{h\upsilon^2}{2}-\frac{h\tilde{\mathfrak{M}}^2}{2\lambda_2}+\frac{h\mathfrak{M}^{*2}}{2\lambda_2}+b_3\tilde{\upsilon}\hat{\upsilon}^{1+\gamma}\\&+\frac{b_4}{\lambda_2}\tilde{\mathfrak{M}}\hat{\mathfrak{M}}^{1+\gamma}+\mathfrak{a}_2.\end{aligned}\tag{62}$$

According to Lemma 3, we have

$$\left(\frac{h\tilde{\upsilon}^2}{2}\right)^{1-\frac{\gamma}{2}}\leq\mathfrak{A}_4(\gamma)+\frac{h}{2}\tilde{\upsilon}^2\tag{63}$$

$$\left(\frac{h\tilde{\mathfrak{M}}^2}{2\lambda_2}\right)^{1-\frac{\gamma}{2}}\leq\mathfrak{A}_5(\gamma)+\frac{h}{2\lambda_2}\tilde{\mathfrak{M}}^2\tag{64}$$

where $\mathfrak{A}_4(\gamma)=\frac{\gamma}{2}(1-\frac{\gamma}{2})^{\frac{2-\gamma}{\gamma}}$ and $\mathfrak{A}_5(\gamma)=\frac{\gamma}{2}(1-\frac{\gamma}{2})^{\frac{2-\gamma}{\gamma}}$.

According to [42], one yields $x(y-x)^{\nu}\leq\frac{\nu}{1+\nu}(y^{1+\nu}-x^{1+\nu})$ for $y\geq x$ and $\nu>1$. Similarly, we can obtain

$$\tilde{\upsilon}\hat{\upsilon}^{1+\gamma}\leq\frac{1+\gamma}{2+\gamma}\left(\upsilon^{2+\gamma}-\tilde{\upsilon}^{2+\gamma}\right)\tag{65}$$

$$\tilde{\mathfrak{M}}\hat{\mathfrak{M}}^{1+\gamma}\leq\frac{1+\gamma}{2+\gamma}\left(\mathfrak{M}^{*2+\gamma}-\tilde{\mathfrak{M}}^{2+\gamma}\right).\tag{66}$$

Substituting (63)–(66) into (62) gets

$$\begin{aligned}\dot{V}_3\leq & -\frac{\pi\beta_1}{\gamma T_c\sqrt{\beta_1\beta_2}}V_2^{1-\frac{\gamma}{2}}-\left(\frac{h\tilde{\upsilon}^2}{2}\right)^{1-\frac{\gamma}{2}}-\left(\frac{h\tilde{\mathfrak{M}}^2}{2}\right)^{1-\frac{\gamma}{2}}\\&-\frac{\pi\beta_2}{\gamma T_c\sqrt{\beta_1\beta_2}}2^{\frac{\gamma}{2}}V_2^{1+\frac{\gamma}{2}}-\frac{2^{1+\frac{\gamma}{2}}b_3(1+\gamma)}{2+\gamma}\left(\frac{\tilde{\upsilon}^2}{2}\right)^{1+\frac{\gamma}{2}}\\&-\frac{2^{1+\frac{\gamma}{2}}\lambda_2^{\frac{\gamma}{2}}b_4(1+\gamma)}{2+\gamma}\left(\frac{\tilde{\mathfrak{M}}^2}{2\lambda_2}\right)^{1+\frac{\gamma}{2}}+\mathfrak{a}_3\\\leq & -\frac{\pi}{\gamma T_c\sqrt{\beta_1\beta_2}}\left(\beta_1V_3^{1-\frac{\gamma}{2}}+\beta_2V_3^{1+\frac{\gamma}{2}}\right)+\mathfrak{a}_3\end{aligned}\tag{67}$$

where $\mathfrak{a}_3=\mathfrak{a}_2+\mathfrak{A}_4(\gamma)+\mathfrak{A}_5(\gamma)+\frac{h\upsilon^2}{2}+\frac{h\mathfrak{M}^{*2}}{2\lambda_2}+b_3\frac{1+\gamma}{2+\gamma}\upsilon^{2+\gamma}+\frac{b_4}{\lambda_2}\frac{1+\gamma}{2+\gamma}\mathfrak{M}^{*2+\gamma}$.

TABLE I
MODEL PARAMETERS

Symbol	Value	Unit	Symbol	Value	Unit
M	1.0750	kg	g	9.8	m/s^2
D_p	0.0071	N/V	D_y	0.022	N/V
l_a	0.002	m	K_{pp}	0.0011	N·m/V
K_{py}	0.0021	N·m/V	K_{yp}	−0.0027	N·m/V
K_{yy}	0.0022	N·m/V	J_p	0.0215	kg·m^2
J_y	0.0237	kg·m^2			

Consequently, it can be concluded from (67) and Lemma 5 that the 2-DOF helicopter system is PPTS. In addition, the tracking error will converge to a sufficiently small region, i.e.,

$$\Delta = \left\{ \lim_{t\to T_p} e \mid V_3 \le \min\left\{ \left(\frac{2\gamma T_c\sqrt{\beta_1\beta_2}}{\pi\beta_1}\right)^{\frac{2}{2-\gamma}}, \left(\frac{2\gamma T_c\sqrt{\beta_1\beta_2}}{\pi\beta_2}\right)^{\frac{2}{2+\gamma}} \right\} \right\} \tag{68}$$

within a PT T_p that satisfies $T_p < T_{\max} = \sqrt{2}T_c$. Then, it can be confirmed from (24) and (25) that the virtual controller α is bounded. Furthermore, in the light of the Lyapunov function of V_1, V_2 and V_3, we can get the filter error s and the estimation error $\tilde{\sigma}, \tilde{\varrho}$ and $\tilde{\upsilon}$ are all bounded in PT. Similarly, the boundedness of the control signal μ can be obtained from (43) and (44).

Nextly, it will be proved that the Zeno behavior can be avoided in the proposed control method. Since the control input $\tau_i(t)$ is bounded, one has $\frac{c_i|\tau_i(t)|+n_i}{\max\{|\dot{\mu}_i(t)|,m_i\}}$ is also bounded. Then, it can be easily concluded that there exists a lower bound of the time interval between two successive triggering that satisfies $t_i^* = t_{q+1}^i - t_q^i > 0$, which also imply that the Zeno effect is avoided. This completes the proof. ■

IV. SIMULATION RESULT

This section presents some simulation results for demonstrating the effectiveness of the proposed control method. The 2-DOF helicopter model parameters are displayed in Table I.

Feasibility verification: For the investigated 2-DOFHS, the initial conditions are chosen as $\mathcal{K}_1(0) = [0, 0]^T$ (rad/s). In addition, the desired trajectories $\mathcal{K}_d$ are assumed as $\mathcal{K}_d = [(\pi/9) \times \sin(t), (\pi/18) \times \sin(t)]^T$ (rad/s). The system uncertainty is given as $\Delta A(\mathcal{K}) = 0.1A(\mathcal{K})$. The external disturbance $\bar{d}$ is set as $\bar{d} = [\sin(t), \cos(t)]^T$. The design parameters are chosen as $\delta_j = 0.02, \tau_{j\min} = 0.02, c_i = 0.8, n_i = 0.2, m_i = 100, T_c = 10s, \xi = 1, \lambda_1 = 40, \lambda_2 = 40, \gamma = 0.8, \mathfrak{b}_1 = 1, \mathfrak{b}_2 = 1.5, \mathfrak{c} = 1, \epsilon_1 = 0.05, \epsilon_2 = 0.05, \mathfrak{e} = 0.01,$ and $\overline{\Delta} = 0.1 \times e^{-5t}$. The performance function is formulated as

$$\psi_i(t) = \begin{cases} 0.98e^{(-0.1t)}\left(1 - \frac{t}{T_i}\right)^{\frac{5}{2}} + 0.02, & 0 \le t \le 10 \\ 0.02, & t > 10 \end{cases}$$

The Figs. 2–6 display the simulation results. Fig. 2 denotes the system output $\mathcal{K}_1 = [\theta, \phi]^T$ can track the desired signal $\mathcal{K}_d = [\theta_d, \phi_d]^T$ with higher tracking accuracy and faster convergence rate. Fig. 3 describes the system's response trajectories of the tracking error e_{11} and e_{12} with the proposed fixed-time

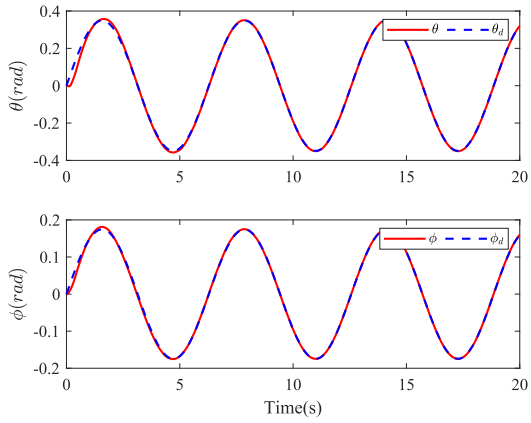

Fig. 2. The trajectories of θ, ϕ and θ_d, ϕ_d.

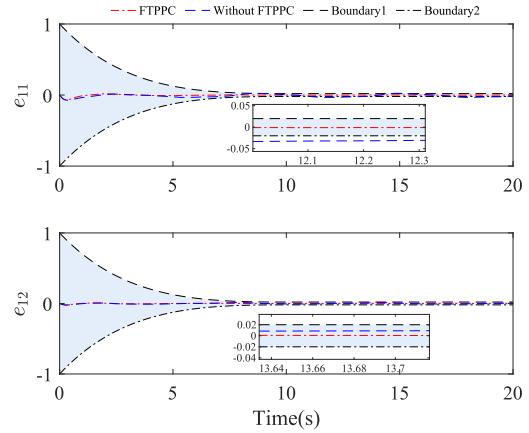

Fig. 3. The tracking errors e_{1i} under different scenarios.

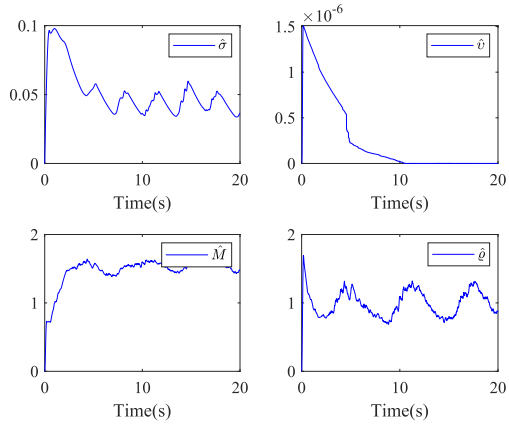

Fig. 4. The adaptive parameters $\hat{\sigma}, \hat{\upsilon}, \hat{\mathfrak{M}}$ and $\hat{\varrho}$.

PPC (FTPPC) strategy and without FTPPC strategy, where the boundary 1 and boundary 2 are the upper and lower boundaries of the performance function, respectively. It can be easily observed that the tracking error can be stringently constrained within a preset area by the proposed control scheme distinct from unconstrained control. Fig. 4 depicts the time response of adaptive parameters $\hat{\upsilon}, \hat{\sigma}, \hat{\varrho}$, and $\hat{\mathfrak{M}}$ under zero initial conditions. The curves of control signals u_1 and u_2 are plotted in Fig. 5. Under the STM, the triggered intervals are displayed in Fig. 6, and the number of the control update are 495 times and 533

TABLE II
PERFORMANCE COMPARISONS UNDER DIFFERENT CONTROL STRATEGIES

Performance indexes	Items	AFPTC in [41]	NAFITC in [14]	NAFTC in [11]	Proposed method
IAE= $\int_0^t \lvert e_{1,i}(\tau)\rvert d\tau$	$e_{1,1}$	0.4485	0.3786	0.5961	0.0913
	$e_{1,2}$	0.1745	0.2408	0.0935	0.0353
ITAE= $\int_0^t t\lvert e_{1,i}(\tau)\rvert d\tau$	$e_{1,1}$	4.3542	4.0421	6.0786	0.3179
	$e_{1,2}$	1.6422	2.3474	0.9570	0.1457

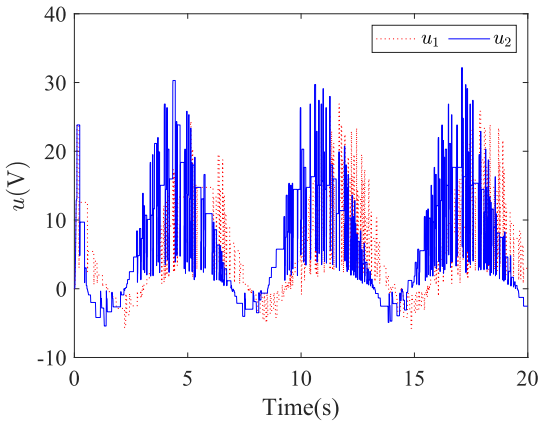

Fig. 5. The control signal u.

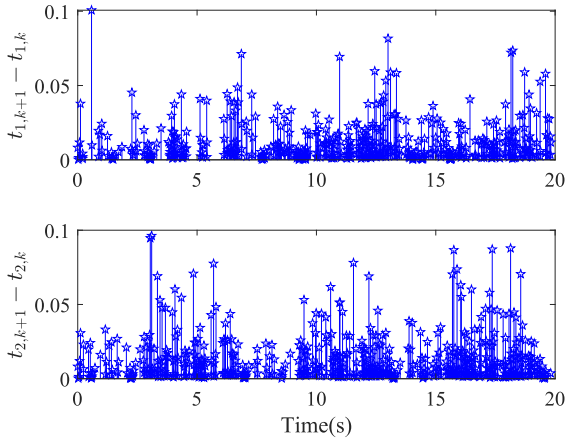

Fig. 6. Triggered intervals $t_{i,k+1}-t_{i,k}$.

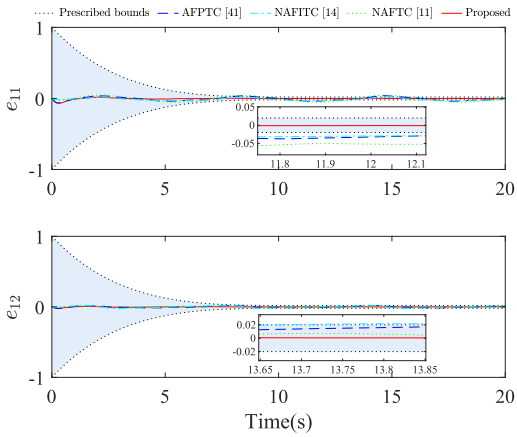

Fig. 7. The curves of tracking errors $e_{1,i}(i=1,2)$ under different control methods.

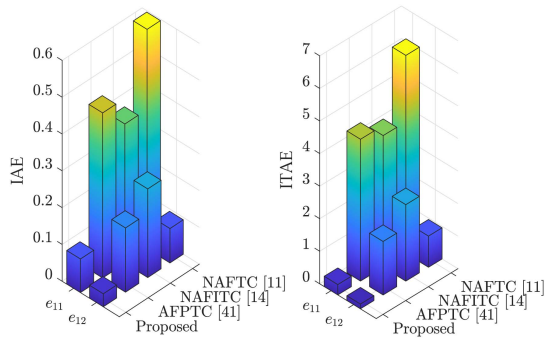

Fig. 8. IAE and ITAE under different control methods.

times, respectively. According to the simulation results, one can obtain that the proposed neural adaptive quantized self-triggered controller ensures that the tracking error can be regulated into a preset area in a PT obeying an appointed tracking performance, and a relative balance between tracking performance and control costs can be achieved.

*Comparative Analysis:*In this section, some comparative results are given to illustrate the proposed control scheme's superiority in comparison to some existing schemes including the neural adaptive FTC (NAFTC) scheme in [11], the neural adaptive fixed-time control (NAFITC) scheme in [14] and the adaptive fuzzy predefined-time control (AFPTC) scheme in [41]. The initial information and system parameters are selected to be identical in order to guarantee the comparative simulation rigor. The simulation results under different control schemes about the trajectories of the tracking errors $e_{1,i}(i=1,2)$ are plotted by Fig. 7. Furthermore, although the NAFTC, NAFITC and AFPTC schemes guarantee the tracking errors are driven to a small domain of the origin, the proposed control scheme achieves better PT convergence of the tracking errors and transient steady-state performance. In addition, in order to quantitative evaluation under different control methods of the control performance, the performance indexes about integral time-weighted absolute error (ITAE) $=\int_0^t t\lvert e_{i,1}(\tau)\rvert d\tau$ and IAE $=\int_0^t \lvert e_{i,1}(\tau)\rvert d\tau$ are adopted, in light of Table II. Then, Fig. 8 shows the comparison results.

Furthermore, the event-triggered mechanism (ETM) developed in [33] is employed to show the differences between the proposed STC and the existing ETC. The comparison results are provided in Table III. It follows from Table III that the proposed STC strategy effectively improves the utilization of

TABLE III
TRIGGER TIMES UNDER DIFFERENT COMMUNICATION PROTOCOLS

Items	Trigger times		Variation
	ETM in [33]	The proposed STC method	
τ_1	790	495	37.11%
τ_2	693	533	23.09%

communication resources without the need for continuous monitoring of trigger condition in comparison to the ETM presented in [33].

Remark 4: Noted that the steady time T_a of the NAFTC proposed in [11] depends on the initial value $V(x(0))$. Compared with NAFTC, the setting time of NAFITC in [14] is governed only by the design parameters without the need to rely on the initial states. Nevertheless, it should be pointed out that the setting time T_b of NAFITC is described by a complex function. Distinct from the NAFITC, the settling time of the proposed method is determined by a given parameter T_c rather than a nonintuitive function expression.

V. CONCLUSION

In this article, a PT neural adaptive quantized self-triggered control method has been developed for a 2-DOFHS with guaranteed tracking performance. In the recursive control procedure, a fixed-time performance function and a predefined-time filter have been utilized to achieve the preassigned constraint on the tracking performance and predefined convergence of the filter errors, respectively. Meanwhile, an adaptive quantized self-triggered controller is proposed, where the input quantization and self-triggered mechanism are integrated to release the bandwidth burden to a greater extend on the premise of performance assurance. The obtained results have indicated that the proposed control strategy can ensure that all the signals in the CLS are PPTB and the tracking error can converge to a preassigned region satisfying an appointed performance. Finally, the effectiveness and superiority of the proposed control strategy have been demonstrated by the simulation results. Considering the significance of secure control against malicious cyber-attacks and trade-off between system performance and control costs, motivated by the results reported in [44], [45], the reinforcement learning-based adaptive predefined-time optimal secure control issue for 2-DOF helicopters subject to deception attacks will be further investigated in our future work.

REFERENCES

[1] A. Karimoddini, H. Lin, B. M. Chen, and T. H. Lee, "Hybrid three-dimensional formation control for unmanned helicopters," *Automatica*, vol. 49, no. 2, pp. 424–433, Feb. 2013.

[2] A. Ailon and S. Arogeti, "Closed-form nonlinear tracking controllers for quadrotors with model and input generator uncertainties," *Automatica*, vol. 54, pp. 317–324, Apr. 2015.

[3] S. M. Schlanbusch and J. Zhou, "Adaptive backstepping control of a 2-DOF helicopter system in the presence of quantization," in *Proc. 9th Int. Conf. Control, Mechatron. Autom.*, 2021, pp. 110–115.

[4] H. Zhang and J. Liu, "Event-triggered fuzzy flight control of a two-degree-of-freedom helicopter system," *IEEE Trans. Fuzzy Syst.*, vol. 29, no. 10, pp. 2949–2962, Oct. 2021.

[5] M. Chen, K. Yan, and Q. Wu, "Multiapproximator-based fault-tolerant tracking control for unmanned autonomous helicopter with input saturation," *IEEE Trans. Syst. Man Cybern. Syst.*, vol. 52, no. 9, pp. 5710–5722, Sep. 2022.

[6] Z. Zhao, J. Zhang, Z. Liu, C. Mu, and K. S. Hong, "Adaptive neural network control of an uncertain 2-DOF helicopter with unknown backlash-like hysteresis and output constraints," *IEEE Trans. Neural Netw. Learn. Syst.*, vol. 34, no. 12, pp. 10018–10027, Dec. 2023.

[7] M. Mokhtari, "Adaptive neural network-based dynamic surface control for a 3-DoF helicopter," *J. Control Autom. Elect. Syst.*, vol. 35, pp. 326–336, Mar. 2024.

[8] B. Tian, H. Lu, Z. Zuo, Q. Zong, and Y. Zhang, "Multivariable finite-time output feedback trajectory tracking control of quadrotor helicopters," *Int. J. Robust Nonlinear Control*, vol. 28, no. 1, pp. 281–295, Jan. 2018.

[9] X. Wang, Z. Li, X. Yu, and Z. He, "Adaptive smooth disturbance observer-based fast finite-time attitude tracking control of a small unmanned helicopter," *J. Franklin Inst.*, vol. 359, no. 11, pp. 5322–5340, Jul. 2022.

[10] Y. Ren, D. Liu, Z. Zhao, and C. K. Ahn, "Finite-time anti-disturbance control of an information-constrained autonomous helicopter flexible slung-load system with compound disturbance," *Aerosp. Sci. Technol.*, vol. 140, 2023, Art. no. 108417.

[11] Z. Zhao, J. Zhang, S. Chen, W. He, and K. S. Hong, "Neural-network-based adaptive finite-time control for a two-degree-of-freedom helicopter system with an event-triggering mechanism," *IEEE/CAA J. Automatica Sinica*, vol. 10, no. 8, pp. 1754–1765, Aug. 2023.

[12] A. Polyakov, "Nonlinear feedback design for fixed-time stabilization of linear control systems," *IEEE Trans. Autom. Control*, vol. 57, no. 8, pp. 2106–2110, Aug. 2012.

[13] Y. Huang, M. Zhu, Z. Zheng, and M. Feroskhan, "Fixed-time autonomous shipboard landing control of a helicopter with external disturbances," *Aerosp. Sci. Technol.*, vol. 84, pp. 18–30, Jan. 2019.

[14] Z. Zhao, J. Wu, C. Mu, Y. Liu, and K. S. Hong, "Neural-network-based adaptive fixed-time control for a 2-DOF helicopter system with input quantization and output constraints," *IEEE Trans. Neural Netw. Learn. Syst.*, early access, May 29, 2024, doi: 10.1109/TNNLS.2024.3403145.

[15] H. Ma, R. Ren, F. Tao, Z. Fu, and N. Wang, "FTDO-based adaptive fuzzy fixed-time tracking control for uncertain unmanned helicopter with output constraints," *Aerosp. Sci. Technol.*, vol. 147, 2024, Art. no. 109019.

[16] Y. Zhang, M. Chadli, and Z. Xiang, "Predefined-time adaptive fuzzy control for a class of nonlinear systems with output hysteresis," *IEEE Trans. Fuzzy Syst.*, vol. 31, no. 8, pp. 2522–2531, Aug. 2023.

[17] H. Wang, M. Tong, X. Zhao, B. Niu, and M. Yang, "Predefined-time adaptive neural tracking control of switched nonlinear systems," *IEEE Trans. Cybern.*, vol. 53, no. 10, pp. 6538–6548, Oct. 2023.

[18] T. Zhang, R. Bai, and Y. Li, "Practically predefined-time adaptive fuzzy quantized control for nonlinear stochastic systems with actuator dead zone," *IEEE Trans. Fuzzy Syst.*, vol. 31, no. 4, pp. 1240–1253, Apr. 2023.

[19] S. Xie, Q. Chen, and X. He, "Predefined-time approximation-free attitude constraint control of rigid spacecraft," *IEEE Trans. Aerosp. Electron. Syst.*, vol. 59, no. 1, pp. 347–358, Feb. 2023.

[20] H. Xu, D. Yu, and Y. Liu, "Observer-based fuzzy adaptive predefined time control for uncertain nonlinear systems with full-state error constraints," *IEEE Trans. Fuzzy Syst.*, vol. 32, no. 3, pp. 1370–1382, Mar. 2024.

[21] C. P. Bechlioulis and G. A. Rovithakis, "Robust adaptive control of feedback linearizable MIMO nonlinear systems with prescribed performance," *IEEE Trans. Autom. Control*, vol. 53, no. 9, pp. 2090–2099, Oct. 2008.

[22] S. Shao, L. Wang, X. Yan, and Q. Wu, "Trajectory planning and prescribed performance tracking control based on fractional-order observers for unmanned helicopters with unmeasurable states," *Aerosp. Sci. Technol.*, vol. 139, Dec. 2023, Art. no. 108360.

[23] Z. Zhao, J. Wu, Z. Liu, W. He, and C. L. P. Chen, "Adaptive neural network control of a 2-DOF helicopter system considering input constraints and global prescribed performance," *Sci. China Inf. Sci.*, vol. 67, 2024, Art. no. 172202.

[24] H. Shen, X. Yu, H. Yan, J. H. Park, and J. Wang, "Robust fixed-time sliding mode attitude control for a 2-DOF helicopter subject to input saturation and prescribed performance," *IEEE Trans. Transp. Electrific.*, early access, May 17, 2024, doi: 10.1109/TTE.2024.3402316.

[25] Z. Liu, F. Wang, Y. Zhang, and C. L. Philip Chen, "Fuzzy adaptive quantized control for a class of stochastic nonlinear uncertain systems," *IEEE Trans. Cybern.*, vol. 46, no. 2, pp. 524–534, Feb. 2016.

[26] S. M. Schlanbusch, J. Zhou, and R. Schlanbusch, "Adaptive attitude control of a rigid body with input and output quantization," *IEEE Trans. Ind. Electron.*, vol. 69, no. 8, pp. 8296–8305, Aug. 2022.

[27] Z. Ye, D. Zhang, J. Cheng, and Z. Wu, "Event-triggering and quantized sliding mode control of UMV systems under DoS attack," *IEEE Trans. Veh. Technol.*, vol. 71, no. 8, pp. 8199–8211, Aug. 2022.

[28] Z. Zhao, J. Zhang, Z. Liu, W. He, and K.-S. Hong, "Adaptive quantized fault-tolerant control of a 2-DOF helicopter system with actuator fault and unknown dead zone," *Automatica*, vol. 148, no. 2, 2023, Art. no. 110792.

[29] G. Zhang, S. Liu, J. Huang, and W. Zhang, "Dynamic event-triggered path-following control of underactuated surface vehicle with the experiment verification," *IEEE Trans. Veh. Technol.*, vol. 71, no. 10, pp. 10415–10425, Oct. 2022.
[30] K. Yu, Y. Li, Z. Peng, and S. Tong, "Distributed event-triggered formation control of planar vehicles without velocity sensors," *IEEE Trans. Veh. Technol.*, vol. 72, no. 3, pp. 2988–3000, Mar. 2023.
[31] X. Cai et al., "Event-triggered control strategy for 2-DoF helicopter system under DoS attacks," *IEEE Trans. Transp. Electrific.*, vol. 9, no. 2, pp. 3240–3254, Jun. 2023.
[32] C. K. Verginis, C. P. Bechlioulis, A. G. Soldatos, and D. Tsipianitis, "Robust trajectory tracking control for uncertain 3-DOF helicopters with prescribed performance," *IEEE/ASME Trans. Mechatron.*, vol. 27, no. 5, pp. 3559–3569, Oct. 2022.
[33] Z. Zhao, J. Zhang, Z. Liu, H. Li, and C. L. P. Chen, "Event-triggered adaptive neural fault-tolerant control for a 2-DOF helicopter system with prescribed performance," *Automatica*, vol. 162, 2024, Art. no. 111511.
[34] G. Cui, H. Xu, J. Yu, and H.-K. Lam, "Event-triggered distributed fixed-time adaptive attitude control with prescribed performance for multiple QUAVs," *IEEE Trans. Automat. Sci. Eng.*, vol. 21, no. 3, pp. 4471–4481, Jul. 2024.
[35] W. Liu, C.-C. Lim, P. Shi, and S. Xu, "Backstepping fuzzy adaptive control for a class of quantized nonlinear systems," *IEEE Trans. Fuzzy Syst.*, vol. 25, no. 5, pp. 1090–1101, Oct. 2017.
[36] Z. Chen, Z. Li, and C. L. P. Chen, "Adaptive neural control of uncertain MIMO nonlinear systems with state and input constraints," *IEEE Trans. Neural Netw. Learn. Syst.*, vol. 28, no. 6, pp. 1318–1330, Jun. 2017.
[37] C. Wang, L. Guo, C. Wen, Q. Hu, and J. Qiao, "Event-triggered adaptive attitude tracking control for spacecraft with unknown actuator faults," *IEEE Trans. Ind. Electron.*, vol. 67, no. 3, pp. 2241–2250, Mar. 2020.
[38] M. Chen, P. Shi, and C.-C. Lim, "Adaptive neural fault-tolerant control of a 3-DOF model helicopter system," *IEEE Trans. Syst. Man Cybern. Syst.*, vol. 46, no. 2, pp. 260–270, Feb. 2016.
[39] S. Song, J. H. Park, B. Zhang, and X. Song, "Adaptive NN finite-time resilient control for nonlinear time-delay systems with unknown false data injection and actuator faults," *IEEE Trans. Neural Netw. Learn. Syst.*, vol. 33, no. 10, pp. 5416–5428, Oct. 2022.
[40] Z. Zuo and L. Tie, "Distributed robust finite-time nonlinear consensus protocols for multi-agent systems," *Int. J. Syst. Sci.*, vol. 47, no. 6, pp. 1366–1375, 2016.
[41] S. Xie, Q. Chen, and Q. Yang, "Adaptive fuzzy predefined-time dynamic surface control for attitude tracking of spacecraft with state constraints," *IEEE Trans. Fuzzy Syst.*, vol. 31, no. 7, pp. 2292–2304, Jul. 2023.
[42] Y. Sun and L. Zhang, "Fixed-time adaptive fuzzy control for uncertain strict feedback switched systems," *Inf. Sci.*, vol. 546, pp. 742–752, 2021.
[43] M. M. Polycarpou, "Stable adaptive neural control scheme for nonlinear systems," *IEEE Trans. Autom. Control*, vol. 41, no. 3, pp. 447–451, Mar. 1996.
[44] G. Cui, H. Xu, S. Xu, and J. Gu, "Predefined-time adaptive fuzzy bipartite consensus control for multi-quadrotors under malicious attacks," *IEEE Trans. Fuzzy Syst.*, vol. 32, no. 4, pp. 2187–2197, Apr. 2024.
[45] G. Wen, R. Zhou, Y. Zhao, and B. Niu, "Optimized backstepping combined with dynamic surface technique for single-input-single-output nonlinear strict feedback system," *IEEE Trans. Syst. Man Cybern. Syst.*, vol. 54, no. 7, pp. 4210–4221, Jul. 2024.

Xiaona Song (Senior Member, IEEE) received the Ph.D. degree in control science and engineering from the Nanjing University of Science and Technology, Nanjing, China, in 2011. From February 2009 to August 2009, April 2016 to April 2017, and July 2019 to August 2019, she was a Visiting Scholar with the Department of Electrical Engineering, Utah State University, Logan, UT, USA, Southern Illinois University Carbondale, Carbondale, IL, USA, and Yeungnam University, Gyeongsan, South Korea, respectively. Since 2011, she has been with the Henan University of Science and Technology, Luoyang, China, where she is currently a Professor with the School of Information Engineering. Her research interests include reaction-diffusion systems, adaptive and learning control of flexible systems, cooperative control and optimization of unmanned systems.

Longbo Chu received the B.S. degree in electronic science and technology from the School of Mechanical and Electrical Engineering, Henan Institute of Science and Technology, Xinxiang, China, in 2022. He is currently working toward the master's degree in control engineering with the School of Information Engineering, Henan University of Science and Technology, Luoyang, China. His research interests include adaptive and learning control for unmanned helicopter systems.

Zhijia Zhao (Member, IEEE) received the B.Eng. degree in automatic control from the North China University of Water Resources and Electric Power, Zhengzhou, China, in 2010, and the M.Eng. and Ph.D. degrees in automatic control from the South China University of Technology, Guangzhou, China, in 2013 and 2017, respectively. He is currently a Professor with the School of Mechanical and Electrical Engineering, Guangzhou University, Guangzhou. His research interests include adaptive and learning control, flexible mechanical systems, and robotics.

Shuai Song (Member, IEEE) received the M.S. degree in control engineering from the Henan University of Science and Technology, Luoyang, China, in 2017, and the Ph.D. degree in control science and engineering from the Nanjing University of Science and Technology, Nanjing, China, in 2021. From 2019 to 2020, he was a Visiting Scholar with the Department of Electrical Engineering, Yeungnam University, Gyeongsan, South Korea. Since 2021, he has been with the Henan University of Science and Technology, Luoyang, China, where he is currently an Associate Professor with the School of Information Engineering. His research interests include adaptive and learning control for nonlinear systems, and cooperative formation control of unmanned systems.

Keum-Shik Hong (Life Fellow, IEEE) received the B.S. degree in mechanical design and production engineering from Seoul National University, Seoul, South Korea, in 1979, the first M.S. degree in mechanical engineering from Columbia University, New York, NY, USA, in 1987, and the second M.S. degree in applied mathematics and the Ph.D. degree in mechanical engineering from the University of Illinois at Urbana-Champaign, Champaign, IL, USA, in 1991. He was with the School of Mechanical Engineering, Pusan National University, Busan, South Korea, during 1993–2022, and has been a Professor Emeritus since 2022. His Integrated Dynamics and Control Engineering Laboratory was a National Research Laboratory designated by the Ministry of Science and Technology of Korea in 2003. In 2009, under the auspices of the World Class University Program of the Ministry of Education, Science, and Technology of Korea, he established the Department of Cogno-Mechatronics Engineering, PNU. He holds a Distinguished Professorship with the Institute For Future, School of Automation, Qingdao University, Qingdao, China. His research interests include autonomous vehicles, brain-computer interface, nonlinear systems theory, adaptive control, distributed parameter systems, and innovative control applications in brain engineering. He is a Fellow of the Korean Academy of Science and Technology, ICROS Fellow, Member of the National Academy of Engineering of Korea, and many other societies. Dr. Hong was an Associate Editor for *Automatica* (2000–2006), and Editor-in-Chief of the *Journal of Mechanical Science and Technology* (JMST, 2008–2011) and *International Journal of Control, Automation, and Systems* (IJCAS, 2018–2022). He was a past President of the Institute of Control, Robotics and Systems (ICROS), Korea, and Asian Control Association (2020-21). He was the recipient of the Presidential Award of Korea (2007) and Service Merit Medal of Korea (2022) from the Korean government. His academic awards include the Best Paper Award from the KFSTS of Korea (1999) and IEEE Academic Award (2016).